ESAIM: M2AN 44 (2010) 1255–1277
DOI: 10.1051/m2an/2010025

ESAIM: Mathematical Modelling and Numerical Analysis
www.esaim-m2an.org

NUMERICAL MODELLING OF ALGEBRAIC CLOSURE MODELS OF OCEANIC TURBULENT MIXING LAYERS

Anne-Claire Bennis[1], Tomas Chacón Rebollo[2], Macarena Gómez Mármol[2] and Roger Lewandowski[1]

Abstract. We introduce in this paper some elements for the mathematical and numerical analysis of algebraic turbulence models for oceanic surface mixing layers. In these models the turbulent diffusions are parameterized by means of the gradient Richardson number, that measures the balance between stabilizing buoyancy forces and destabilizing shearing forces. We analyze the existence and linear exponential asymptotic stability of continuous and discrete equilibria states. We also analyze the well-posedness of a simplified model, by application of the linearization principle for non-linear parabolic equations. We finally present some numerical tests for realistic flows in tropical seas that reproduce the formation of mixing layers in time scales of the order of days, in agreement with the physics of the problem. We conclude that the typical mixing layers are transient effects due to the variability of equatorial winds. Also, that these states evolve to steady states in time scales of the order of years, under negative surface energy flux conditions.

Mathematics Subject Classification. 76D05, 35Q30, 76F65, 76D03.

Received May 4, 2008. Revised November 17, 2009.
Published online March 17, 2010.

1. Introduction

This paper is devoted to the mathematical and numerical analysis of turbulence models of surface oceanic mixing layers. In a context of global climate change, the accurate simulation of the Surface Sea Temperature (SST) is of primary importance, as it affects the global oceanic circulation, and has a deep impact in the evolution of polar ices (*cf.* Goose *et al.* [6]). This problem has been analyzed by the physical oceanography community since the early 80's. One of their main objectives is to build mathematical models to achieve a right numerical simulation of SST, mainly in Tropical Ocean areas, as these areas receive large amounts of solar heat that is brought into the oceanic global energy balance.

The parameterization of turbulence in the mixing layer must take into account the two forces that act in the momentum and mass exchange produced by mixing effects: buoyancy and shear. The early class of models

Keywords and phrases. Turbulent mixing layers, Richardson number, first order closure models, conservative numerical solution, stability of steady states, tests for tropical seas.

[1] IRMAR, Université de Rennes 1, Campus de Beaulieu, 35042 Rennes Cedex, France.
[2] Departamento de Ecuaciones Diferenciales y Análisis Numerico, Universidad de Sevilla, C/Tarfia, s/n. 41080, Sevilla, Spain. chacon@us.es

parameterize the turbulent viscous and diffusion in terms of the Richardson number by means of algebraic expressions. The Richardson number measures the rate between stabilizing buoyancy forces and destabilizing shearing forces. One of the most popular of these models was introduced by Pacanowski and Philander in 1981 [13]. This description in terms of the Richardson number allows large mixing in zones of low stratification, and inhibits it in zones of strong stratification. This model was modified in several ways, in order to obtain a better fitting with experimental measurements. One of these improvements was proposed by Gent in 1991 (*cf.* [5]). Another kind of improvements was based upon the parameterization of the vertical profile of turbulent kinetic energy (KPP model, *cf.* Large *et al.* [9]). All these are vertical 1D models based upon the knowledge of the atmospheric forcing to set the boundary conditions. More classical turbulence models of k-ε kind, have also been developed, taking into account buoyancy effects. Let us mention for instance the second order closure models of Mellor and Yamada [12] and Gaspar *et al.* [4].

In the recent years, the mathematical community has shown an increasing interest in the theoretical and numerical analysis of geophysical flow problems. This interest has been mainly addressed to models for large-scale atmospheric and oceanic flows, frequently using shallow water approaches. In the case of water flows, rather little attention has been addressed to buoyant turbulence effects. However, the behavior of SST deeply depends on a correct description of the turbulent mass and momentum mixing in the upper oceanic layer, where buoyancy plays a key role.

There are several relevant questions concerning mixing layer models that may be analyzed in mathematical terms. The main one is to determine whether they provide accurate numerical predictions of the flow in the upper oceanic layer, as this is the purpose of these models. This requires to determine whether these models are mathematically well posed problems and whether their numerical approximations are stable and provide approximate solutions close to the theoretical solutions.

Another relevant issue is to analyze the mathematical stability of physically stable configurations. These configurations correspond to decreasing density profiles, associated to well-mixed turbulent layers and so to stable distribution of mass and momentum, and are typical in tropical oceans. A right numerical simulation of such configurations only will be possible if they are mathematically stable.

A third mathematical issue of interest is the analysis of existence and stability of mathematical equilibria of the mixing-layer models, and their relationship with the above-referenced well-mixed layer configurations. This requires to determine whether these configurations are steady solutions of the models, and if not, whether well-mixed layers are intermediate transient states between initial conditions and mathematical equilibria.

The mathematical analysis of these models faces hard difficulties. This mainly occurs because the turbulent diffusions depend on the gradients of the unknowns. Energy methods fail to obtain estimates of approximated solutions in norms strong enough (typically, these should be of $W^{2,p}$ kind) to handle the gradients in compactness or fixed-point arguments to prove existence of solutions. An alternative to this technique is provided by the Semigroup Theory for parabolic evolution equations, which in addition allows to analyze the asymptotic stability in time. In Potier-Ferry [15] this theory is applied to the analysis of stability of equilibria solutions of non-linear second order parabolic equations, with Dirichlet boundary conditions. Under smoothness conditions for the coefficients, existence of short-time solutions is proved, if the initial condition is close to an equilibrium. Furthermore, the linearization principle is applied to analyze the asymptotic stability: If the linearized equation around a given equilibrium is exponentially stable, then the above solution of the non-linear equation exists for all times, and converges exponentially to the equilibrium.

Our purpose in this paper is to give some mathematical and numerical insight to the analysis of the algebraic Richardson number-based models mentioned above. We use Potier-Ferry's theory as a guide to answer to some of the questions set above. Although this theory is not directly applicable to our mixing-layer models, because these includes non-linear Neumann boundary conditions, we assume the working hypothesis that the linearization principle also holds under these conditions. With this guiding line, after introducing the standard Richardson number-based mixing layers that we consider (Sect. 2), we perform an analysis of existence of equilibrium solutions in Section 3. We prove that these are not the well-mixed mixing layer configurations, but linear profiles for velocity and density. We also introduce a new model that allows unstable initial profiles,

which cannot be simulated by the standard models. We next prove the linear stability of these equilibria states for physically stable configurations of the layer, in Section 4. Thus, if Potier-Ferry's theory holds in our case, this guarantees the exponential stability of the equilibria states, and the existence and uniqueness of solutions for initial conditions close enough to the equilibria.

In Section 5 we analyze a typical conservative numerical scheme used by the physical oceanography community to solve mixing-layer models. We prove that this scheme is well suited, in the sense that it is stable (in low-order norms) and verify a maximum principle. However, we do not prove stability in $W^{2,p}$ norm, that would allow to bound the gradients of the approximate solutions, and then would allow to prove the convergence of the scheme.

Section 6 is devoted to the numerical tests where we use realistic initial and boundary data measured in tropical seas. We observe that the typical mixing-layer configurations are reproduced by all models considered, with characteristic formation times of about two days. We also observe that the theoretical equilibria are indeed reached by our numerical models. Further, we observe that mixing-layer configurations asymptotically evolve to the theoretical equilibria, with characteristic times of one and a half year. We finally test the new model introduced with initial conditions that include unstable initial density profiles: It also simulates the formation of a typical mixing layer. In the context of Potier-Ferry's theory, we interpret these results in the sense that well-mixed configurations are transient states lying in the attraction domain of stable equilibria, for a large class of initial conditions that includes unstable density profiles, under negative surface energy flux conditions.

We analyze a simplified model in Section 7, in order to show the ability of Potier-Ferry's theory to analyze our problem. This model applies to one single unknown (the vertical derivative of the density) and satisfies Dirichlet boundary conditions. We prove that Potier-Ferry's theory may be applied in this case: a wide range of stable equilibria are proved to be exponentially stable.

We present our conclusions in Section 8. We interpret our results in terms of Potier-Ferry's theory, and guess how this theory should be extended to give a complete answer to the questions set above.

2. Setting of model problems

The wind-stress generates intense mixing processes in a layer below the ocean surface. This layer has two parts, the upper one is a homogeneous layer, known as the mixed layer. This layer presents almost-constant temperature (and salinity). The bottom of the mixed layer corresponds to the top of the pycnocline, a thin layer with a large gradient of density. For instance, in tropical seas a sharp thermocline is formed. In this last layer still mixing processes do occur, but it has not a homogeneous structure. The zone formed by the two layers is known as the mixing layer. Its thickness may vary between ten meters and a few hundred meters, depending on the latitude. It also presents seasonal variations.

Typically, the variables used to describe the mixing layer are the statistical means of horizontal velocity (u, v) and density ρ. In the ocean, the density is a function of temperature and salinity through a state equation. So, we consider the density as an idealized thermodynamic variable which is intended to represent temperature and salinity variations. We are mainly interested in tropical seas, where the salinity in the mixing layer is almost constant, and the density is just a function of the temperature.

The mixed layer being strongly dominated by vertical fluxes, velocity, density and pressure are supposed to be horizontally homogeneous. We assume

$$U = (u(z,t), v(z,t), w(z,t)), \quad \rho = \rho(z,t), \quad p = p(z,t).$$

This leads to one-dimensional models depending only on the vertical variable. The Coriolis force is neglected, a good approximation in tropical oceans because this force is small in equatorial regions (*cf.* [14]). Therefore, the equations governing the mixing layer, obtained by statistical averaging of Navier-Stokes equations, are

$$\begin{cases} \partial_t u - \alpha_1 \, \partial_{zz} u = -\partial_z \langle u' \, w' \rangle \,, \\ \partial_t v - \alpha_1 \, \partial_{zz} v = -\partial_z \langle v' \, w' \rangle \,, \\ \partial_t \rho - \alpha_2 \, \partial_{zz} \rho = -\partial_z \langle \rho' \, w' \rangle \,, \end{cases} \tag{2.1}$$

where $(u', v'), w', \rho'$ represent the fluctuations of the horizontal velocity, vertical velocity and density, and α_1, α_2 are the laminar viscosity and diffusion. The notation $\langle\ \ \rangle$ signifies that the quantity is statistically averaged, in the usual sense used in turbulence modelling. Equations (2.1) are the classical equations corresponding to a modelling of a water column. Equations (2.1) are not closed. To close them, the vertical fluxes appearing in the right-hand side need to be modelled.

The Richardson number-based models use the concept of eddy diffusion in order to represent turbulent fluxes. So we set

$$-\langle u'\, w'\rangle = \nu_{T1}\partial_z u, \quad -\langle v'\, w'\rangle = \nu_{T1}\partial_z v, \quad -\langle \rho'\, w'\rangle = \nu_{T2}\partial_z \rho.$$

ν_{T1} and ν_{T2} are the vertical eddy viscosity and diffusivity coefficients. This modelling corresponds to statistically stationary turbulence and thus to well-mixed layers. The eddy coefficients are expressed as functions of the gradient Richardson number R defined as

$$R = -\frac{g}{\rho_0}\,\frac{\partial_z \rho}{(\partial_z u)^2 + (\partial_z v)^2},$$

where g is the gravitational acceleration and ρ_0 a reference density (for example $\rho_0 = 1025$ kg·m^{-3}).

The gradient Richardson number is the ratio between the stabilizing vertical forces due to buoyancy and the destabilizing horizontal ones due to shear in a water column.

When $R >> 1$, a strongly stratified layer takes place. This corresponds to a stable configuration. When $0 < R << 1$, a slightly stratified layer takes place. This corresponds to a configuration with low stability. The case $R < 0$ corresponds to a configuration statically unstable ($\partial_z \rho > 0$), that in fact we are not modelling because it does not correspond to statistically stable turbulence. However, we must handle this situation for our numerical experiments, in order to take into account initial conditions with unstable configurations that should evolve to stable configurations as the layer becomes well-mixed. A simple way is to set large constant values for the turbulent diffusions in this case, although we shall need a smoother modelling for our analysis.

The set of equations, initial and boundary conditions governing the mixing layer can now be written

$$\begin{cases} \partial_t u - \partial_z\,(\nu_1 \partial_z u) = 0, \\ \partial_t v - \partial_z\,(\nu_1 \partial_z v) = 0, \\ \partial_t \rho - \partial_z\,(\nu_2 \partial_z \rho) = 0, \ \text{for } t \geqslant 0 \text{ and } -h \leqslant z \leqslant 0, \\ u = u_b,\ v = v_b,\ \rho = \rho_b \ \text{ at the depth } z = -h, \\ \nu_1 \partial_z u = \dfrac{\rho_a}{\rho_0} V_x,\ \nu_1 \partial_z v = \dfrac{\rho_a}{\rho_0} V_y,\ \nu_2 \partial_z \rho = Q \ \text{ at the surface } z = 0, \\ u = u_0,\ v = v_0,\ \rho = \rho_0 \ \text{ at initial time } t = 0. \end{cases} \tag{2.2}$$

In system (2.2), $\nu_1 = \alpha_1 + \nu_{T1}$, $\nu_2 = \alpha_2 + \nu_{T2}$ respectively are the total viscosity and diffusion. The constant h denotes the thickness of the studied layer that must contain the mixing layer. Therefore the circulation for $z < -h$, under the boundary layer, is supposed to be known, either by observations or by a deep circulation numerical model. This justifies the choice of Dirichlet boundary conditions at $z = -h$, $(u_b,\ v_b)$ and ρ_b being the values of horizontal velocity and density in the layer located below the mixed layer. The forcing by the atmosphere is modelled by the fluxes at the sea-surface: V_x and V_y are respectively the stress exerced by the zonal wind-stress and the meridional wind-stress and Q represents the thermodynamical fluxes, heating or cooling, precipitations or evaporation. We have $(V_x, V_y) = C_D\,|U^a|\,U^a$, where $U^a = (u_a, v_a)$ is the air velocity and C_D $(= 1.2 \times 10^{-3})$ is a friction coefficient (*cf.* Kowalik and Murty [8]).

We describe hereafter the modelling of the eddy coefficients made by the Pacanowski-Philander (PP) (*cf.* [13]) and Gent (*cf.* [5]) models. We write $\nu_1 = f_1(R)$ and $\nu_2 = f_2(R)$. In PP model, the functions f_1 and f_2 are defined as

$$f_1(R) = \alpha_1 + \frac{\beta_1}{(1+5R)^2}, \quad f_2(R) = \alpha_2 + \frac{f_1(R)}{1+5R} = \alpha_2 + \frac{\alpha_1}{1+5R} + \frac{\beta_1}{(1+5R)^3}. \tag{2.3}$$

This formulation has been used in the OPA code developed by Paris 6 University by Delecluse and co-workers (*cf.* [1,10]) with coefficients

$$\alpha_1 = 1\times 10^{-6},\ \beta_1 = 1\times 10^{-2},\ \alpha_2 = 1\times 10^{-7}\ \left(\text{units: m}^2\cdot\text{s}^{-1}\right).$$

The selection criterion for the coefficients appearing in these formulas was the best agreement of numerical results with observations carried out in different tropical areas.

A variant of formulation (3), proposed by Gent [5], is

$$f_1(R) = \alpha_1 + \frac{\beta_1}{(1+10R)^2}, \quad f_2(R) = \alpha_2 + \frac{\beta_2}{(1+10R)^3} \tag{2.4}$$

with $\alpha_1 = 1\times 10^{-4},\ \beta_1 = 1\times 10^{-1},\ \alpha_2 = 1\times 10^{-5},\ \beta_2 = 1\times 10^{-1}$(units: $\text{m}^2\cdot\text{s}^{-1}$). A formulation similar to (2.4) when replacing $10R$ by $5R$ and varying the values of the coefficients α_1, α_2 between the surface and the depth 50 m is used in Goose *et al.* [6].

These models apply to vertically stable configurations, for which $\partial_z \rho \le 0$, and thus $R \ge 0$. Turbulence may be generated by the shear induced by the wind and by buoyancy forces, but the model describes the state of the flow once the vertical configuration has been stabilized by buoyancy forces. However, as we already have mentioned, for numerical simulations the case $R \le 0$, that corresponds to unstable buoyant configurations, must be taken into account.

The main physical reason for the structure of f_1 in (2.3) and (2.4) is that buoyancy stratification inhibits mixing effects, and that this inhibition increases as R increases. Moreover, mixing effects should tend to disappear as R tends to infinity. This suggests a structure for the turbulent viscosity as

$$\nu_{T1} = \frac{\beta}{(1+a\,R)^m}, \quad \text{for some} \quad \beta > 0,\ a > 0,\ m > 0.$$

Also, the expression for f_2 in (2.3) and (2.4) follows from experimental measurements: ν_{T2}/ν_{T1} decreases to zero as R increases. This suggests a similar modelling, although this one is less clear than that of ν_{T1}. A possibility is provided by Gent's model:

$$\nu_{T2} = \beta' \frac{\nu_{T1}}{(1+a\,R)^{m'}}, \quad \text{for some} \quad \beta' > 0,\ m' > 0.$$

A similar behavior is yield by Pacanowski-Philander's model,

$$\nu_{T2} = \beta' \frac{\alpha_1 + \nu_{T1}}{(1+a\,R)^{m'}}.$$

The experimental origins of this modelling may be found in Jones [7] and Robinson [16].

3. Equilibria states

We determine in this section the equilibria of system (2.2). Our analysis is based upon the application of the linearization principle to quasi-linear parabolic equations with data depending on the gradient of the unknown developed in Potier-Ferry [15]. In this work, the evolution PDE problem is viewed as an abstract differential equation upon a convenient abstract Banach space X:

$$\frac{\mathrm{d}u(t)}{\mathrm{d}t} + T(u(t))\,u(t) = f(u(t)), \tag{3.1}$$

where $T(u)$ is a family of operators that have a domain D that is dense on X and independent on u. Fixed-point theory is used to prove local existence in time and uniqueness for smooth enough initializations close enough to some equilibrium. The linearization principle is used to prove the asymptotic exponential stability of equilibrium solutions. Essentially, this principle states that if the linearized equation around an equilibrium is asymptotically exponentially stable, then it is also exponentially non-linearly stable. This theory is applied to the non-linear heat equation with homogeneous Dirichlet boundary conditions, by choosing the spaces D and X as

$$D = W^{2,p}(\Omega) \cap W_0^{1,p}(\Omega), \qquad X = L^p(\Omega),$$

where p is larger than the dimension d of the open set Ω where the PDE problem is set. This ensures that the gradients of the unknowns are bounded functions, thus handling one of the main difficulties of the problem.

Potier-Ferry's theory applies to Dirichlet boundary conditions, and not to the non-linear Neumann boundary conditions that appear in problem (2.2). We shall assume as working hypothesis that the linearization principle also applies to these conditions. This is likely, by a convenient use of linearization techniques and fixed-point theory.

Potier-Ferry's theory supports the interest of calculating the equilibria of problem (2.2) and studying its linear stability, that we analyze in the present and the next sections. We prove in this section that all equilibria are linear profiles for both velocity and pressure associated to some fixed Richardson number R. We prove in the next section that these equilibria are linearly exponentially stable if $R > 0$, corresponding to physically stable configurations of the mixing-layer. Thus, if Potier-Ferry's theory could be extended to our non-linear boundary conditions, our results would yield the exponential stability of all physically stable equilibria.

The equilibria of problem (2.2) are given by the following:

Theorem 3.1. *Assume that the algebraic equation*

$$R = -g\,\frac{\rho_0}{\rho_a^2}\,\frac{Q}{V_x^2 + V_y^2}\,\frac{\left(f_1(R)\right)^2}{f_2(R)} \tag{3.2}$$

admits at least a solution R^e. Then, for each solution R^e there exists a unique associated equilibrium solution of problem (2.2) in $[H^1(-h,0)]^3$, given by

$$u^e(z) = u_b + \frac{V_x \rho_a}{\rho_0 f_1(R^e)}\,(z+h), \tag{3.3}$$

$$v^e(z) = v_b + \frac{V_y \rho_a}{\rho_0 f_1(R^e)}\,(z+h), \tag{3.4}$$

$$\rho^e(z) = \rho_b + \frac{Q}{f_2(R^e)}\,(z+h). \tag{3.5}$$

Proof. Assume at first that we are looking for smooth equilibria of system (2.2) (at least with C^2 regularity). These equilibria satisfy the PDE system

$$\begin{cases} \partial_z u \left(f_1\left(R\right) \partial_z u\right) = 0, \\ \partial_z u \left(f_1\left(R\right) \partial_z v\right) = 0, \\ \partial_z u \left(f_2\left(R\right) \partial_z \rho\right) = 0. \end{cases} \tag{3.6}$$

Integration with respect to z yields:

$$\begin{cases} f_1\left(R\right) \partial_z u = \dfrac{V_x \rho_a}{\rho_0}, \\ f_1\left(R\right) \partial_z v = \dfrac{V_y \rho_a}{\rho_0}, \\ f_2\left(R\right) \partial_z \rho = Q. \end{cases} \tag{3.7}$$

As $R = -\dfrac{g}{\rho_0} \dfrac{\partial_z \rho}{\left(\partial_z u\right)^2 + \left(\partial_z v\right)^2}$, we deduce that R satisfies the algebraic equation (3.2). Then, for each solution R^e of this equation we obtain an equilibrium solution of problem (2.2) (including the boundary conditions) given by (3.3)–(3.5). Indeed, as R^e, $f_1(R^e)$ and $f_2(R^e)$ do not depend on z, we deduce these equilibrium profiles by integration in z of equations (3.7).

Let us now prove the uniqueness of this solution in $[H^1(-h,0)]^3$. Assume that (u_1^e, v_1^e, ρ_1^e) is another equilibrium associated to R^e belonging to $[H^1(-h,0)]^3$. Then, the difference in the first component of the velocity $U = u^e - u_1^e$ weakly satisfies

$$\partial_z U \left(f_1\left(R^e\right) \partial_z U\right) = 0, \quad \nu_1 \partial_z U = 0 \quad \text{at} \quad z = -h, \quad \text{and} \quad U = 0 \quad \text{at} \quad z = 0;$$

this is

$$\int -h^0 f_1(R^e) \partial_z U \partial_z V = 0, \quad \forall V \in H^1(-h,0) \quad \text{such that} \quad V(0) = 0.$$

Then, $U = 0$. Similarly, $v^e = v_1^e$, and $\rho^e = \rho_1^e$. □

Remark 3.1. It is relevant to observe that statically stable configurations, associated to positive Richardson numbers, here appear associated to negative heat fluxes Q. It is also relevant to remark that this equation admits a meaningful physical interpretation: at equilibrium the ratio between potential and turbulent kinetic energy is proportional to the surface fluxes ratio,

$$\frac{\text{Potential energy}}{\text{Turbulent kinetic energy}}(\text{Equilibrium}) = \text{Constant}\left(R^e\right) \times \frac{Q}{V_x^2 + V_y^2}.$$

We next analyze the existence of solutions of equation (3.2). These solutions may be interpreted as the intersection of the curves

$$k\left(R\right) = \frac{\left(f_1\left(R\right)\right)^2}{f_2\left(R\right)} \quad \text{and} \quad h\left(R\right) = CR, \quad \text{with} \quad C = -\frac{\rho_a^2 (V_x^2 + V_y^2)}{gQ\rho_0}.$$

For each actual model, the existence and the number of equilibria only depends on the value of the constant C, or, more specifically, of the fluxes ratio

$$r = \frac{Q}{V_x^2 + V_y^2}.$$

PP and Gent models present the same qualitative behavior. We recall that these models are no more valid respectively for $R \leq \hat{R}$ with $\hat{R} = -1/5$ and $\hat{R} = -1/10$ since the diffusion f_2 at these ranges is negative.

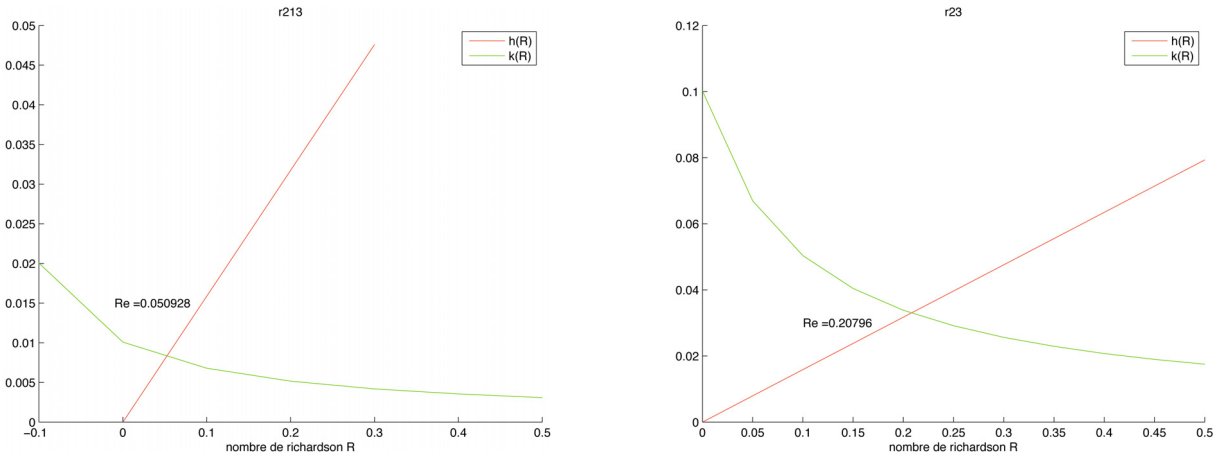

FIGURE 1. Solution of the equation for equilibrium Richardson numbers for PP (left) and Gent models (right). (Figure in color available online at www.esaim-m2an.org.)

For each one of these models, $k(R)$ is a strictly decreasing function for $R \geq 0$. This yields a unique equilibrium state for $R > 0$, which corresponds to statically stable configurations.

There is also a range $0 \geq R > R^*$, for which equation (3.2) admits several solutions. This range corresponds to non-equilibrium profiles which, as we already mentioned, are not modelled. However, to handle initial conditions with possibly non-stable configurations, that should evolve to well-mixed layers by buoyancy and turbulent shear, it is convenient to devise models that also yield positive eddy diffusions for negative Richardson numbers. With this purpose, we introduce in this paper a new model, which is a slight modification of PP model. This model is given by

$$f_1(R) = \alpha_1 + \frac{\beta_1}{(1+5R)^2}, \quad f_2(R) = \alpha_2 + \frac{f_1(R)}{(1+5R)^2}, \tag{3.8}$$

with the same constants as the PP model. This new model has a unique equilibrium R^e for any fluxes ratio r. As we shall see in the numerical tests, this model gives solutions very close to those provided by the PP model.

In the sequel we shall use the abridged notation Rijk to define each one of the three models we are considering. The indices i, j and k represent the exponents of the denominators in the definition of the turbulent diffusions f_1 and f_2. Thus, R213, R224 and R23 will respectively denote the PP, Gent and new models.

As an example, we present the equilibria Richardson numbers corresponding to realistic values (see Sect. 6.1). We have taken $V_x = 35\times10^{-3}$ m^2·s^{-2}, $V_y = 97\times10^{-5}$ m^2·s^{-2}, and also a negative Q, $Q = -1\times10^{-6}$ kg·m^{-2}·s^{-1}, so we are in a situation of static stability.

We observe on Figures 1 and 2 the only equilibrium solution corresponding to each model. From Figure 2 it is clear that there exists a unique equilibrium solution for the new model, for any value of the fluxes ratio r.

4. Linear stability of equilibrium solutions

In this section, we analyze the stability of the equilibrium solutions. We prove that for all the three models considered, these equilibria are linearly stable for negative fluxes ratio r. By Potier-Ferry's theory, this supports the well-posedness of all these models, for physically meaning equilibrium solutions.

Let us consider an initial perturbation of the form

$$(u_0, v_0, \rho_0) = (u^e, v^e, \rho^e) + (u_0', v_0', \rho_0'),$$

where (u^e, v^e, ρ^e) is an equilibrium solution, and (u_0', v_0', ρ_0') is a small perturbation.

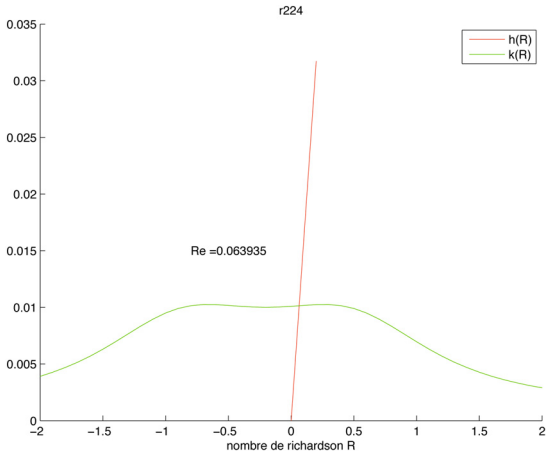

FIGURE 2. Solution of the equation for equilibrium Richardson numbers for new model. (Figure in color available online at www.esaim-m2an.org.)

We assume that at time t, the solution of our model (2.1) has the structure

$$(u, v, \rho) = (u^e, v^e, \rho^e) + (u', v', \rho').$$

Let us introduce the new variables $\theta = \partial_z \rho$, $\alpha = \partial_z u$ and $\beta = \partial_z v$. The Richardson number, in terms of these variables, is

$$R = -\frac{g}{\rho_0} \frac{\theta}{(\alpha^2 + \beta^2)} = R(\alpha, \beta, \theta),$$

and consequently the turbulent diffusions are functions of (α, β, θ). Then, the equations satisfied by the perturbation are

$$\begin{cases} \partial_t u' - \partial_z \left(f_1(\alpha, \beta, \theta) \left(\alpha^e + \alpha' \right) \right) = 0, \\ \partial_t v' - \partial_z \left(f_1(\alpha, \beta, \theta) \left(\beta^e + \beta' \right) \right) = 0, \\ \partial_t \rho' - \partial_z \left(f_2(\alpha, \beta, \theta) \left(\theta^e + \theta' \right) \right) = 0. \end{cases} \tag{4.1}$$

Set $\mathcal{F} = f_1(\alpha, \beta, \theta) - f_1(\alpha^e, \beta^e, \theta^e)$ and $\mathcal{G} = f_2(\alpha, \beta, \theta) - f_2(\alpha^e, \beta^e, \theta^e)$. Taylor expansion yields

$$\mathcal{F} = (\alpha - \alpha^e) \frac{\partial f_1}{\partial \alpha}(\alpha^e, \beta^e, \theta^e) + (\beta - \beta^e) \frac{\partial f_1}{\partial \beta}(\alpha^e, \beta^e, \theta^e) + (\theta - \theta^e) \frac{\partial f_1}{\partial \theta}(\alpha^e, \beta^e, \theta^e) + \dots \tag{4.2}$$

and

$$\mathcal{G} = (\alpha - \alpha^e) \frac{\partial f_2}{\partial \alpha}(\alpha^e, \beta^e, \theta^e) + (\beta - \beta^e) \frac{\partial f_2}{\partial \beta}(\alpha^e, \beta^e, \theta^e) + (\theta - \theta^e) \frac{\partial f_2}{\partial \theta}(\alpha^e, \beta^e, \theta^e) + \dots \tag{4.3}$$

Let us denote, for $k = 1, 2$: $f_k^e = f_k(\alpha^e, \beta^e, \theta^e)$,

$$\left(\frac{\partial f_k}{\partial \alpha} \right)^e = \frac{\partial f_k}{\partial \alpha}(\alpha^e, \beta^e, \theta^e), \left(\frac{\partial f_k}{\partial \beta} \right)^e = \frac{\partial f_k}{\partial \beta}(\alpha^e, \beta^e, \theta^e), \left(\frac{\partial f_k}{\partial \theta} \right)^e = \frac{\partial f_k}{\partial \theta}(\alpha^e, \beta^e, \theta^e).$$

We next replace f_1 and f_2 by their Taylor expansions (Eqs. (4.2) and (4.3)) in the equation satisfied by the perturbation (4.1), and neglect the second order terms. This yields a linear system of the form

$$\partial_t v - M \partial_{zz} V = 0, \tag{4.4}$$

where

$$M = \begin{pmatrix} f_1^e + \alpha^e \left(\frac{\partial f_1}{\partial \alpha}\right)^e & \alpha^e \left(\frac{\partial f_1}{\partial \beta}\right)^e & \alpha^e \left(\frac{\partial f_1}{\partial \theta}\right)^e \\ \beta^e \left(\frac{\partial f_1}{\partial \alpha}\right)^e & f_1^e + \beta^e \left(\frac{\partial f_1}{\partial \beta}\right)^e & \beta^e \left(\frac{\partial f_1}{\partial \theta}\right)^e \\ \theta^e \left(\frac{\partial f_2}{\partial \alpha}\right)^e & \theta^e \left(\frac{\partial f_2}{\partial \beta}\right)^e & f_2^e + \theta^e \left(\frac{\partial f_2}{\partial \theta}\right)^e \end{pmatrix}, \quad V = \begin{pmatrix} u' \\ v' \\ \rho' \end{pmatrix}. \tag{4.5}$$

Linear stability will follow if all eigenvalues λ_k of M, $k = 1, 2, 3$ have positive real parts. Indeed, this will ensure that the initial perturbation in the linearized system is exponentially damped as $t \to +\infty$ and its solution will converge to the steady solution.

To verify that all the λ_k have positive real parts, it is enough to prove that three independent invariants of matrix M are positive. A lengthy calculation yields

$$\mathrm{Trace}(M) = 2f_1(R) + f_2(R) + R(f_2'(R) - 2f_1'(R));$$

$$\mathrm{Det}(M) = f_1(R)(f_1(R)f_2(R) + Rf_1(R)f_2'(R) - 2Rf_2(R)f_1'(R));$$

$$\mathrm{Trace}(\mathrm{Adj}M) = 2f_1(R)f_2(R) + 2f_1(R)Rf_2'(R) - 2f_2(R)Rf_1'(R) + f_1(R)^2 - 2f_1(R)Rf_1'(R).$$

Some algebra shows that all of them are strictly positive for the three models we are considering, when $R > 0$. Thus, we conclude that all these models are linearly stable for $R > 0$.

Also, for each model we also obtain a small range of negative Richardson numbers, for which it is linearly stable. This is a rather surprising result, as these ranges correspond to physically unstable configurations. We may consider that this is due to the structure of the functions modelling the eddy diffusions, and that only solutions in a neighborhood of equilibria corresponding to $R > 0$ could be considered meaningful.

5. Numerical discretization

We have analyzed the stability of a standard conservative semi-implicit discretization of the PDEs appearing in model (2.1). We discretize initially by piecewise affine finite elements. This next yields a conservative finite difference discretization by using quadrature formulae to approximate the non-linear integrals. This is the kind of discretization used in practice by physical oceanographers (*cf.* [3,8,10]).

To describe it, assume that the interval $[-h, 0]$ is divided into N subintervals of length $\Delta z = h/(N-1)$, with nodes $z_i = -(i-1)\,h\,\Delta z$, $i = 1, \ldots, N-1$, and construct the finite element space

$$V_\Delta = \{ w_\Delta \in C^0([-h, 0]) \,|\, w_{\Delta|_{]z_{i-1}, z_i[}} \text{ is affine, } i = 1, \ldots, N;\ w_\Delta(-h) = 0 \}. \tag{5.1}$$

The equation for u, for instance, is discretized by linearization of f_1 as

$$\text{Obtain} \quad u_\Delta \in u_b + V_\Delta \quad \text{such that}$$

$$(P_\Delta) \quad \int_{-h}^{0} \frac{u_\Delta^{n+1} - u_\Delta^n}{\Delta t}\, w_\Delta + \int_{-h}^{0} f_1(R_\Delta^n)\, \partial_z u_\Delta^{n+1} \partial_z w_\Delta = L^{n+1}(w_\Delta), \quad \forall w_\Delta \in V_\Delta, \tag{5.2}$$

where $L^{n+1}(w_\Delta) = \dfrac{\rho_a}{\rho_0} V_x^{n+1}\, w_\Delta(0)$.

We also consider the non-linear method

$$\text{Obtain} \quad u_\Delta \in u_b + V_\Delta \quad \text{such that}$$

$$(Q_\Delta) \quad \int_{-h}^{0} \frac{u_\Delta^{n+1} - u_\Delta^n}{\Delta t}\, w_\Delta + \int_{-h}^{0} f_1(R_\Delta^{n+1})\, \partial_z u_\Delta^{n+1} \partial_z w_\Delta = L^{n+1}(w_\Delta), \quad \forall w_\Delta \in V_\Delta, \tag{5.3}$$

which bears better asymptotic properties (see Sect. 5.2).

This discretization is stable under the hypothesis that the turbulent viscosity f_1 is uniformly bounded and positive:

$$\text{There exist} \quad 0 < \nu \le M \quad \text{such that} \quad \nu \le f_1(R) \le M, \quad \forall R \in \mathbb{R}. \tag{5.4}$$

Let us denote by u_Δ the continuous piecewise affine function from $[0,T]$ on to V_Δ whose value in t_n is u_Δ^n, and by L_Δ the piecewise constant in time function whose value in $]t_n, t_{n+1}[$ is L^{n+1}. This function is defined *a.e.* in $[0,T]$. Both u_Δ and L_Δ also depend on Δt, but we prefer this notation for simplicity as it is not confusing.

For simplicity of notation, we shall denote $L^p(L^q)$ the space $L^p((-h,0); L^q(0,T))$ and similarly the spaces $L^p(H^k)$. Our stability result is the following:

Lemma 5.1. *Under hypothesis* (5.4)*, there exists a constant $C > 0$ such that the solution u_Δ of either problem (P_Δ) or (Q_Δ) satisfies*

$$\|u_\Delta\|_{L^\infty(L^2)} + \|u_\Delta\|_{L^2(H^1)} + \|\partial_t u_\Delta\|_{L^2(H^{-1})} \le C\, \|L_\Delta\|_{L^2(H^{-1})}.$$

Note that $\|L_\Delta\|^2_{L^2(H^{-1})} \le \dfrac{\rho_a}{\rho_0}\, C' \displaystyle\sum_{n=1}^{N} \Delta t\, |V_x^{n+1}|^2$.

Proof of Lemma 5.1. The estimates for u_Δ in $L^\infty(L^2)$ and in $L^2(H^1)$ are standard, by taking $w_\Delta = u_\Delta^{n+1}$ and using the identity

$$(a-b)a = \frac{1}{2}|a|^2 - \frac{1}{2}|b|^2 + \frac{1}{2}|a-b|^2, \quad \text{for} \quad a, b \in \mathbb{R}.$$

The estimate for $\partial_t u_\Delta$ is more involved, because as f_1 is not constant, the usual techniques to obtain estimates in $L^2(L^2)$ fail. However, we may obtain estimates in $L^2(H^{-1})$ as follows: Let Π_Δ denote the orthogonal projection from $L^2(-h,0)$ on to V_Δ. As V_Δ is a 1D finite element space with fixed element size, Π_Δ is also stable in $H^1(-h,0)$ (*cf.* [2], Sect. 6): There exists a constant C_1 such that

$$\|\Pi_\Delta w\|_{H^1(-h,0)} \le C_1\, \|w\|_{H^1(-h,0)}, \quad \forall w \in H^1(-h,0). \tag{5.5}$$

Let us consider method (P_Δ). For any $w \in H^1(-h,0)$, and $t \in]t_n, t_{n+1}[$,

$$\begin{aligned} \int_{-h}^{0} \partial_t u_\Delta(t)\, w \;&=\; \int_{-h}^{0} \frac{u_\Delta^{n+1} - u_\Delta^n}{\Delta t}\, \Pi_\Delta w = -\int_{-h}^{0} f_1(R_\Delta^n)\, \partial_z u_\Delta^{n+1} \partial_z \Pi_\Delta w + L^{n+1}(\Pi_\Delta w) \\ &\le\; \left(\|L^{n+1}\|_{H^{-1}(-h,0)} + M\, \|u_\Delta^{n+1}\|_{H^1(-h,0)}\right) \|\Pi_\Delta w\|_{H^1(-h,0)} \\ &\le\; C_1 \left(\|L^{n+1}\|_{H^{-1}(-h,0)} + M\, \|u_\Delta^{n+1}\|_{H^1(-h,0)}\right) \|w\|_{H^1(-h,0)}. \end{aligned} \tag{5.6}$$

The same estimate applies to the implicit method (Q_Δ). We deduce

$$\|\partial_t u_\Delta(t)\|_{H^1(-h,0)} \le C_1 \left(\|L^{n+1}\|_{H^{-1}(-h,0)} + M\, \|u_\Delta^{n+1}\|_{H^1(-h,0)}\right)$$

and we conclude

$$\|\partial_t u_\Delta\|_{L^2(H^{-1})} \le C_2 \left(\|u_\Delta\|_{L^2(H^1)} + \|L_\Delta\|_{L^2(H^{-1})}\right). \qquad \square$$

Let us remark that the issue of the existence of solutions of the implicit method (Q_Δ) is solved with the help of this result. Indeed, it allows to apply a finite-dimensional compactness argument based upon linearization of the equation of the method. We shall not make it explicit for brevity, as it is standard.

To obtain a finite-difference discretization, we approximate the integral of the non-linear term appearing in (P_Δ) or (Q_Δ) by the mid-point rule. However, in practice only the explicit method is used. Denote by φ_i the canonical piecewise affine basis function of V_Δ associated to node z_i; *i.e.*, $\varphi_i(z_j) = \delta ij$. This quadrature formula yields, for the explicit method (P_Δ),

$$\int_{-h}^{0} f_1(R_\Delta^n)\,\partial_z u_\Delta^{n+1}\partial_z\varphi_i \simeq f_1(R_{i-1/2}^n)\frac{u_i^{n+1}-u_{i-1}^{n+1}}{\Delta z} + f_1(R_{i+1/2}^n)\frac{u_i^{n+1}-u_{i+1}^{n+1}}{\Delta z} \tag{5.7}$$

for $i = 2, \ldots, N$, where

$$R_{i-1/2}^n = -\frac{g}{\rho_0}\,\frac{(\rho_i^n-\rho_{i-1}^n)/\Delta z}{\left[|u_i^n-u_{i-1}^n|^2+|v_i^n-v_{i-1}^n|^2\right]/(\Delta z)^2}.$$

Now, applying mass-lumping to the mass integral appearing in (P_Δ) when $w_\Delta = \varphi_i$, we obtain the finite-difference scheme

$$\frac{u_i^{n+1}-u_i^n}{\Delta t} - \frac{f_1(R_{i-1/2}^n)u_{i-1}^{n+1} - \left[f_1(R_{i-1/2}^n)+f_1(R_{i+1/2}^n)\right]u_i^{n+1} + f_1(R_{i+1/2}^n)u_{i+1}^{n+1}}{(\Delta z)^2} = 0. \tag{5.8}$$

For $i = N$, the same procedure yields

$$\frac{u_N^{n+1}-u_N^n}{\Delta t} + f_1(R_{N-1/2}^n)\frac{u_N^{n+1}-u_{N-1}^{n+1}}{\Delta z} = V_1^{n+1}. \tag{5.9}$$

To take into account the discretizations used in practice, we have replaced this equation by a more standard finite difference discretization of the Neumann condition,

$$f_1(R_{N-1/2}^n)\frac{u_N^{n+1}-u_{N-1}^{n+1}}{\Delta z} = V_1^{n+1}. \tag{5.10}$$

This equation allows to compute u_N^{n+1} from u_{N-1}^{n+1}. So we may construct our discretization in terms of the unknowns $U^{n+1} = (u_2^{n+1}, \ldots, u_{N-1}^{n+1})$ and similarly for v and ρ. In matrix form, this discretization reads

$$A^{n+1}\,U^{n+1} = B^{n+1},$$

where A^{n+1} and B^{n+1} respectively are the tridiagonal matrix and the vector array defined with obvious notation by

$$A_{i-1,i}^{n+1} = -\alpha_{i-1/2}^n,\ A_{i,i}^{n+1} = 1+\alpha_{i-1/2}^n+\alpha_{i+1/2}^n,\ A_{i+1,i}^{n+1} = -\alpha_{i+1/2}^n, \quad i = 2, \ldots, N-2;$$

$$A_{N-2,N-1}^{n+1} = -\alpha_{N-3/2}^n, \quad A_{N-1,N-1}^{n+1} = 1+\alpha_{N-3/2}^n;$$

$$B^{n+1} = \left(u_2^n + \alpha_{3/2}^n\,u_b^n, u_3^n, \ldots, u_i^n, \ldots, u_{N-2}^n, u_{N-1}^n + \frac{\Delta t}{\Delta z}\,V_1\right)^t,$$

where

$$\alpha_{i-1/2}^n = \frac{\Delta t}{(\Delta z)^2}\,f_1(R_{i-1/2}^n),$$

and we have included a possibly non-zero Dirichlet boundary condition at $z = -h$: $u_1^n = u_b^n$.

Also, the implicit method (Q_Δ) may be re-written as,

$$A^{n+1}(U^{n+1})\,U^{n+1} = B^{n+1},$$

where $A^{n+1}(U^{n+1})$ is a matrix that depends non-linearly on U^{n+1}, with the same structure of A^{n+1}. The non-linearity is due to the definition of the coefficients $\alpha^n_{i-1/2}$:

$$\alpha^n_{i-1/2} = \frac{\Delta t}{(\Delta z)^2} f_1(R^{n+1}_{i-1/2}).$$

Both discretizations verify a maximum principle:

Lemma 5.2. *If the initial data, u^n_b and V_1 are positive, then u_Δ is positive in $[-h, 0] \times [0, T]$.*

Proof. Let us prove this result for the explicit method (P_Δ). As $f_1 \geq 0$, then A^{n+1} is an M-matrix: It is irreducible, diagonal dominant, strictly for the first line, and all non-diagonal entries are non-positive. Then $(A^{n+1})^{-1}$ has positive entries, and consequently all the u^n_i are positive. □

The same proof applies to the non-linear method (Q_Δ).

5.1. **Equilibria of discrete problems**

A relevant question related to the discrete models introduced is the convergence to the solution of the corresponding continuous models, either for short and long times. We can give some answers to the second case: The equilibria of the continuous and discrete models are the same. Also, the implicit method is asymptotically exponentially stable. Thus, under our working hypothesis upon the validity of Potier-Ferry's theory, this implies the non-linear stability of this method, and the asymptotic convergence of the discrete solutions to the continuous equilibria. We thus obtain a partial result on the convergence of the discrete solutions to the continuous ones.

Our first result is the following:

Theorem 5.1. *The equilibria of the discrete problems (P_Δ) and (Q_Δ) coincide with those of the continuous problem (2.2).*

Proof. The first component of the velocity of equilibria of both discrete problems (P_Δ) and (Q_Δ) are solutions $u_\Delta \in u_b + V_\Delta$ of the equation

$$\int_{-h}^{0} f_1(R_\Delta)\, \partial_z u_\Delta \partial_z w_\Delta = \frac{\rho_a}{\rho_0} V_x w_\Delta(0), \quad \forall w_\Delta \in V_\Delta, \tag{5.11}$$

where

$$R_\Delta = -\frac{g}{\rho_0} \frac{\partial_z \rho_\Delta}{(\partial_z u_\Delta)^2 + (\partial_z v_\Delta)^2},$$

and similar equations for the second component of the velocity $\mathbf{v}_\Delta \in v_b + V_\Delta$ and the density $\rho_\Delta \in \rho_b + V_\Delta$, that we do not detail for brevity.

The first component of the velocity u^e of an equilibrium of the continuous problem is an affine function of z satisfying the boundary condition $u^e(-h) = u_b$. Then, $u^e \in u_b + V_\Delta$. In addition, from the equations satisfied by the continuous equilibria (3.6), we deduce that for any $w \in H^1(-h, 0)$ such that $w(-h) = 0$,

$$\int_{-h}^{0} f_1(R^e) \partial_z u^e \partial_z w = \frac{\rho_a}{\rho_0} V_x w(0).$$

Thus, as $R^e = R_\Delta$, u^e satisfies problem (5.11). The same argument applies to the second component and the density.

This proves that all equilibria of the continuous model are equilibria of the discrete models (P_Δ) and (Q_Δ). To prove that the discrete models do not admit any other equilibria, it is enough to prove that, for fixed R_Δ,

problem (5.11) admits a unique solution. Consider another solution $u'_\Delta \in u_b + V_\Delta$ of this problem. Then, the difference $U_\Delta = u_\Delta - u'_\Delta \in V_\Delta$ satisfies

$$\int_{-h}^{0} f_1(R_\Delta)\, \partial_z U_\Delta \partial_z w_\Delta = 0, \quad \forall w_\Delta \in V_\Delta.$$

Then, $U_\Delta = 0$. The same argument applies for the second component of the velocity and the density. □

5.2. **Linear stability of discrete equilibria**

We prove in this section the exponential linear stability of the implicit discrete model (Q) for positive Richardson numbers. We may also prove the linear stability for the explicit discrete model (P), although we cannot prove that the perturbations decay exponentially to zero. We drop the proof of this result as it is lengthier and lighter.

Theorem 5.2. *The implicit method (Q) is linearly asymptotically exponentially stable.*

Proof. Let us look for u^n_Δ as $u^n_\Delta = u^e + \hat{u}^n_\Delta$, where $\hat{u}^n_\Delta$ is the perturbation. As $u^e \in u_b + V_\Delta$, then $\hat{u}^n_\Delta \in V_\Delta$. Let us also denote

$$Y^n_\Delta = \begin{pmatrix} \hat{u}^n_\Delta \\ \hat{v}^n_\Delta \\ \hat{\rho}^n_\Delta \end{pmatrix} \in V^3_\Delta,$$

where we use similar notations for the perturbations of the second component of the velocity and the density.

Using the Taylor expansion for f_1 and f_2 given by (4.2) and (4.3), from problem (Q) we deduce the following linearized equation for $Y^{n+1}_\Delta \in V^3_\Delta$:

$$\int_{-h}^{0} \frac{Y^{n+1}_\Delta - Y^n_\Delta}{\Delta t} \cdot W_\Delta + \int_{-h}^{0} \left[M\, \partial_z Y^{n+1}_\Delta\right] \cdot \partial_z W_\Delta = 0, \quad \forall W \in V^3_\Delta \tag{5.12}$$

where M is the matrix defined in (4.5), and the dot denotes the Euclidean scalar product in $\mathbb{R}^3$. Notice that Y^{n+1}_Δ satisfies homogeneous Newman boundary conditions at $z = 0$.

Let us take $W_\Delta = Y^{n+1}_\Delta$. Using again the identity $(a-b)\cdot a = \frac{1}{2}|a|^2 - \frac{1}{2}|b|^2 + \frac{1}{2}|a-b|^2$ (where $|\cdot|$ stands for the Euclidean norm in $\mathbb{R}^3$), we deduce

$$\frac{1}{2}\int_{-h}^{0} \left|Y^{n+1}_\Delta\right|^2 - \frac{1}{2}\int_{-h}^{0} |Y^n_\Delta|^2 + \frac{1}{2}\int_{-h}^{0} \left|Y^{n+1}_\Delta - Y^n_\Delta\right|^2 + \Delta t \int_{-h}^{0} \left[M\, \partial_z Y^{n+1}_\Delta\right] \cdot Y^{n+1}_\Delta = 0. \tag{5.13}$$

Notice that $\forall Z \in \mathbb{R}^3$, $[M\, Z] \cdot Z = \left[\bar{M}\, Z\right] \cdot Z$, where $\bar{M} = (M + M^t)/2$. Further, $\bar{M}$ is symmetric and positive definite, as all eigenvalues of M have positive real parts for $R^e > 0$. Then, $\left(\left[\bar{M}\, Z\right] \cdot Z\right)^{1/2}$ is a norm on $\mathbb{R}^3$. Consequently, there exists a constant $C_1 > 0$ such that

$$|Z| \le C_1 \left(\left[\bar{M}\, Z\right] \cdot Z\right)^{1/2}, \quad \forall Z \in \mathbb{R}^3.$$

Combining this estimate with Poincaré inequality, there exists a constant $C_2 > 0$ such that

$$\|Y^{n+1}_\Delta\|^2_{L^2(-h,0)} \le C_P \|\partial_z Y^{n+1}_\Delta\|^2_{L^2(-h,0)} \le C_2 \int_{-h}^{0} \left[M\, \partial_z Y^{n+1}_\Delta\right] \cdot Y^{n+1}_\Delta.$$

Applying this estimate to (5.13),

$$\|Y^{n+1}_\Delta\|^2_{L^2(-h,0)} + \|Y^{n+1}_\Delta - Y^n_\Delta\|^2_{L^2(-h,0)} + C_3\, \Delta t\, \|Y^{n+1}_\Delta\|^2_{L^2(-h,0)} \le \|Y^n_\Delta\|^2_{L^2(-h,0)}, \tag{5.14}$$

for some constant $C_3 > 0$. Then,

$$(1 + C_3\,\Delta t)\sigma_{n+1} \leq \sigma_n, \quad \text{where} \quad \sigma_n = \|Y_\Delta^n\|^2_{L^2(-h,0)}.$$

Consequently,

$$\sigma_{n+1} \leq K\sigma_n \leq \mathrm{e}^{-\gamma\Delta t}\,\sigma_n,$$

where $K = \dfrac{1}{1 + C_3\,\Delta t}$, $\gamma = \mu\, C_3$, for some $\mu \in (0,1)$. So we conclude the exponential asymptotic stability of model (Q):

$$\sigma_n \leq \mathrm{e}^{-\gamma\, n\Delta t}\,\sigma_0 \leq \mathrm{e}^{-\gamma\, t_n}\sigma_0. \qquad \square$$

6. Numerical tests

In this section we perform several numerical tests to analyze the formation of mixed-layers by the numerical models introduced, and their relationship with the equilibria states. We observe that the typical mixing-layer configurations are reproduced by all models considered, with characteristic formation times of about two days. We also observe that the theoretical equilibria are indeed reached by our numerical models. We further observe that mixing-layer configurations asymptotically evolve to the theoretical equilibria, with characteristic times of one and a half year. We finally test the new model introduced with initial conditions that include unstable initial density profiles, that cannot be handled by usual models: It also simulates the formation of a typical mixing layer. In the context of Potier-Ferry's theory, we interpret these results in the sense that well-mixed configurations are transient states lying in the attraction domain of stable equilibria, for a large class of initial conditions that includes unstable density profiles.

We use realistic initial and boundary conditions that correspond to the Equatorial Pacific region called the West-Pacific Warm Pool, located at the equator between 120° E and 180° E. In this region the sea temperature is high and almost constant along the year (28−30 °C). The precipitations are intense and hence the salinity is low.

The initial conditions are taken from the TAO (Tropical Atmosphere Ocean) array (McPhaden [11]), which have been used in many numerical simulations (see the TAO El Niño webpage http://www.pmel.noaa.gov/tao/elnino/simulation.html). The boundary conditions correspond to typical wind stress and heat flux of the West-Pacific Warm Pool.

All the results that we present correspond to the explicit method (P_Δ). We present grid-independent numerical solutions, that remain practically unchanged as the Δz and Δt decrease.

6.1. Case 1: Mixed layer induced by wind stress

This experiment is devoted to test the ability of the numerical method introduced in Section 5 to reproduce the formation of well-mixed boundary layers, for the three considered models (PP, Gent and new one).

We use initial velocity and density profiles measured at 0° N, 165° E for the time period between the 15th June 1991 and the 15th July 1991, displayed in Figure 3. Observe that the initial density profile does not present a mixed layer. The buoyancy flux imposed is -1×10^{-6} kg·m^{-2}·s^{-1} ($\simeq -11$ W·m^{-2}), which is realistic for this region. Indeed, Gent reports in [5] that the heat flux is in the range [0 W·m^{-2}, 20 W·m^{-2}] between 140° E−180° E and 10° S−10° N. Also, the wind stress imposed corresponds to a *zonal wind* (u_1) equal to 8.1 m·s^{-1} (eastward wind) and a *meridional wind* (u_2) equal to 2.1 m·s^{-1} (northward wind). These values are larger than the measured ones, to force the formation of a mixed layer. Figures 4 and 5 display the results corresponding to $t = 48$ h with $\Delta z = 1$ m and $\Delta t = 60$ s. In Figure 4 we represent the whole mixing layer, and in Figure 5, the upper 40 m of this layer. The plots for density profiles show the formation of a mixed layer of some 20 m depth, corresponding to almost constant density values. A pycnocline (strong gradient below a zone where the density is almost constant) is formed below the mixed layer. This is a characteristic density profile for a well-mixed turbulent surface layer. It is striking that the density profiles simulated by the three models

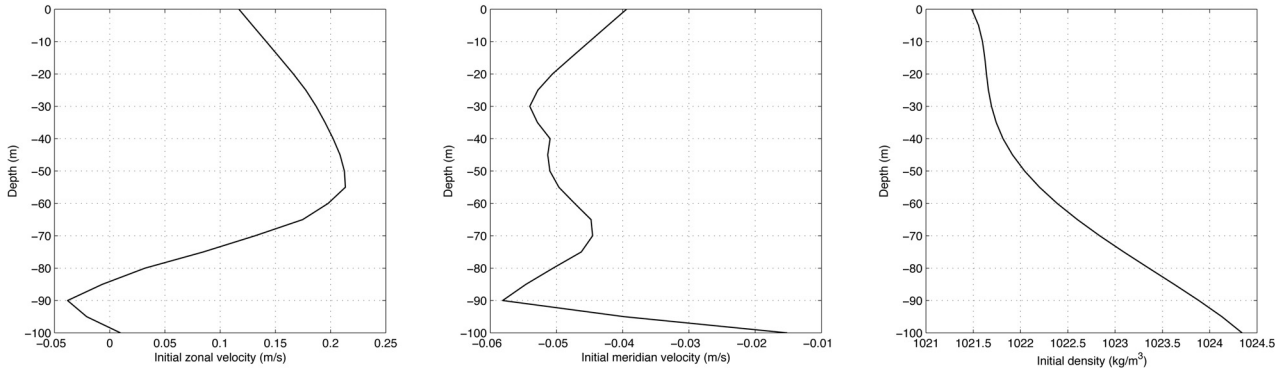

FIGURE 3. Initial zonal velocity, meridian velocity and density profiles (from left to right).

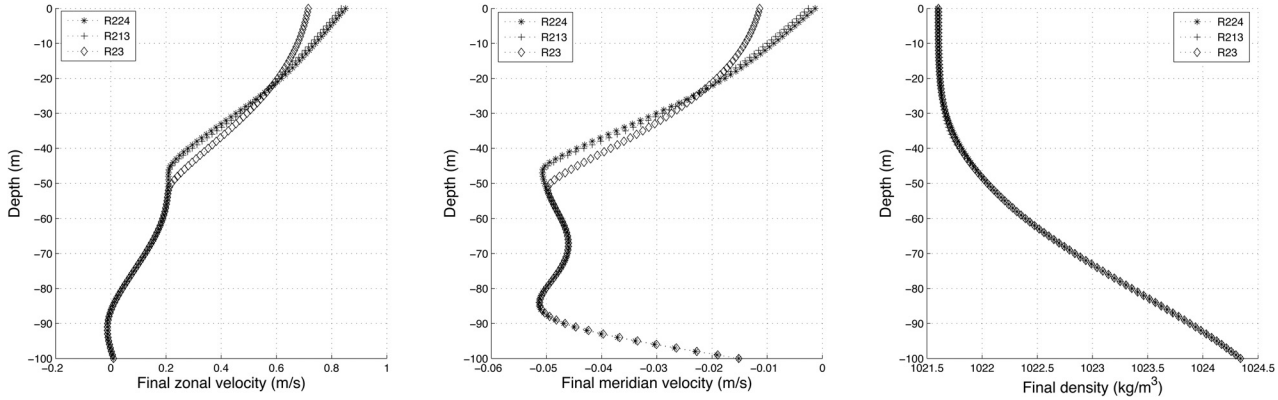

FIGURE 4. Comparison of three turbulence models: R213 (PP), R23 (Gent), R224 (new one). Full mixing layer.

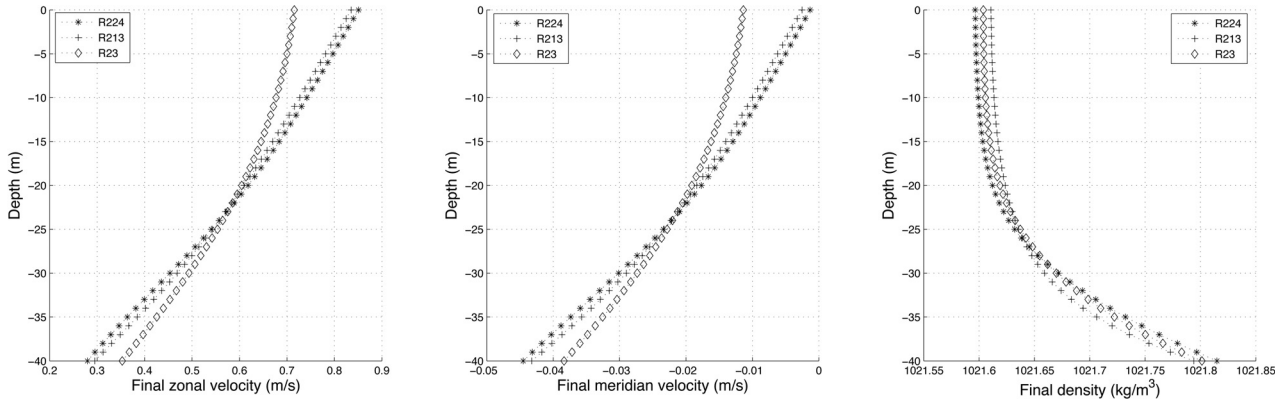

FIGURE 5. Comparison of three turbulence models: R213 (PP), R23 (Gent), R224 (new one). Upper 40 m of mixing layer.

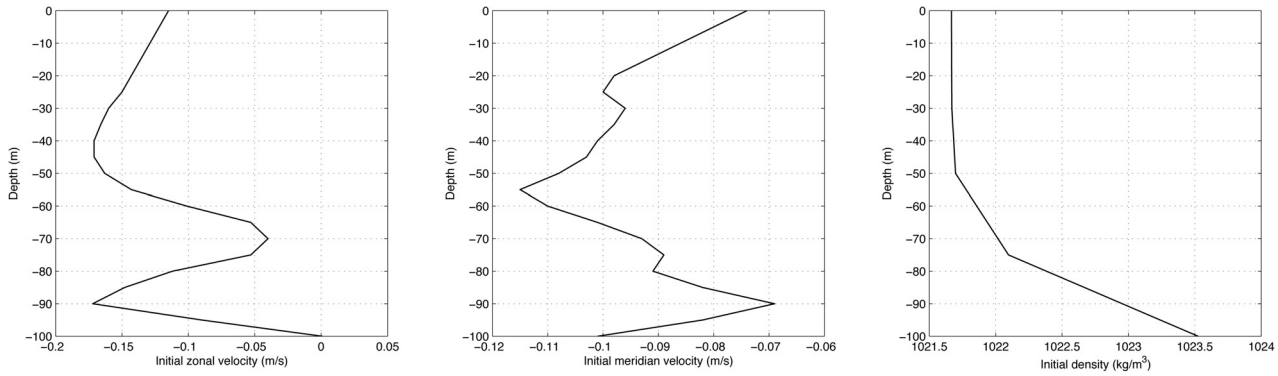

FIGURE 6. Profiles for zonal velocity, meridian velocity and density (from left to right) to test the non-linear stability of all three models.

are quite similar. Velocity and density profiles are quite close for PP and the new model, while the velocity provided by Gent model is somewhat different, mainly near the surface.

From this result we may accept the ability of our numerical method to reproduce the formation of mixing-layers, and also the validity of our new model, as it yields results very close to those of the standard PP model.

6.2. **Case 2: Analysis of non-linear stability of equilibrium solutions**

In this section we investigate by numerical simulation our hypothesis on the applicability of the linearization principle to the analysis of exponential stability. In Section 3 we proved that equilibrium solutions are linearly stable for our three models. Here we analyze whether these equilibria also are non-linearly stable, using real data as initial conditions. Our results indeed show a non-linear stability of equilibria solutions, that act in fact as point-wise attractors whenever we apply a negative buoyancy flux at the surface. In particular, these equilibria attract configurations corresponding to mixing-layers, that appear as transient states reached by the asymptotic evolution of the flow to equilibria. Thus, we obtain some support of our working hypothesis.

The initial profiles represent the ocean mean state on June 17, 1991 (Fig. 6). We have chosen this initial data as the density profile presents a thirty five meters deep mixed layer, and we want to analyze whether this mixed layer evolves to a non-constant density. We have used the following boundary conditions: buoyancy flux $Q = -1 \times 10^{-6}$ kg·m^{-2}·s^{-1} ($\simeq -11$ W·m^{-2}), $u_b = 5.4$ m·s^{-1} (eastward wind) and $v_b = 0.9$ m·s^{-1} (northward wind).

We have run the three models for 10 000 h (about 13 months and a half). The numerical results are displayed in Figure 7. The three turbulence models give linear profiles for the simulated time, with slopes of the same sign. We observe that the velocity for PP and the new model are rather close, while the discrepancy in density is larger. The Gent model presents a larger discrepancy in velocities.

We have observed that the convergence of all models to steady states takes times of the order of several months. This time scale is much larger than that needed to generate a typical homogeneous mixed layer, which is of the order of a few days (in all cases with steady boundary data). This may explain why these linear profiles for the mixing layer are not found in real surface layers, as the boundary data usually change in time scales of the order of hours. Even the formation of a homogeneous mixed layer is not possible if these data change too fast.

Finally, to check that we compute the right steady states, we compare in Figure 8 the solution computed at $t = 10\,000$ h and the theoretical steady state (3.3), (3.4), (3.5), for the new model, corresponding to $R^e = 0.0639$ (see Fig. 2). We observe that both are very close.

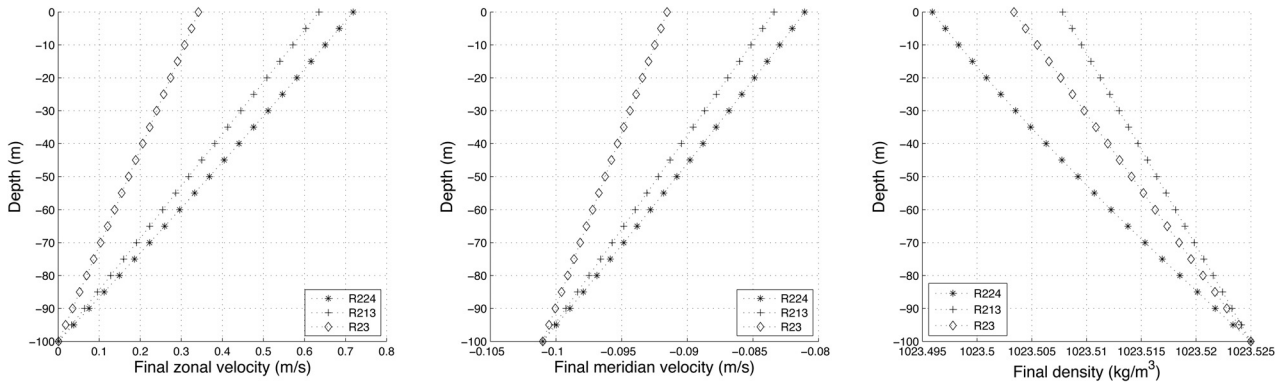

FIGURE 7. Profiles for zonal velocity, meridian velocity and density (from left to right) for all three models, computed at $t = 10\,000$ h.

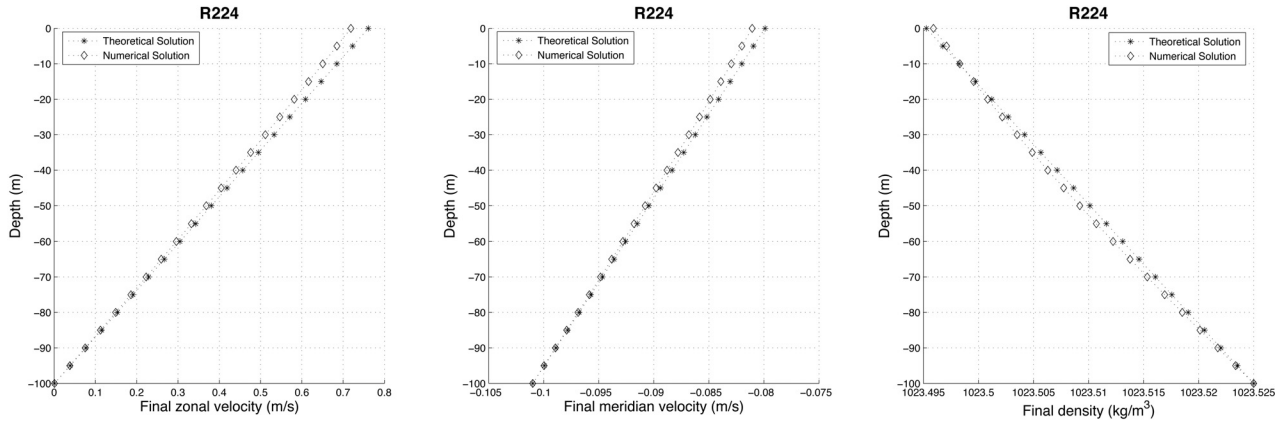

FIGURE 8. Comparison of solution computed at $t = 10\,000$ h *versus* theoretical steady states, for new model (R224).

Several tests with all three models, using different initial data yield qualitative and quantitative similar results. We conclude that the equilibria states are non-linearly stable for negative heat fluxes. Even more, that these equilibria behave as point attractors with associated time scales of the order of the year.

6.3. **Case 3: A static instability zone in the initial density profile**

Although physically stable equilibria correspond to positive Richardson numbers, initial conditions close to some stable equilibrium, but that present vertical instabilities, could asymptotically converge to that equilibrium. This is consistent with the predictions of Potier-Ferry's theory, if the range of attraction of the equilibrium contains such initial conditions. We next present a test that uses real data, in which PP and Gent models cannot be used, as these give negative turbulent diffusions for these data. We instead use the new model, that shows the formation of a homogeneous mixed layer in the typical time scales associated to the formation of these. Thus, the new model may be used to properly simulate the formation of the mixing layer, for a wider range of initial conditions.

In this test we initialize the code with the 17th November 1991 data. The initial profiles are displayed in Figure 9. We observe a seventy meters deep mixed layer, which is not homogeneous in the sense that it is not well mixed. Furthermore, the initial density profile displays a static instability zone between -30 m and -50 m.

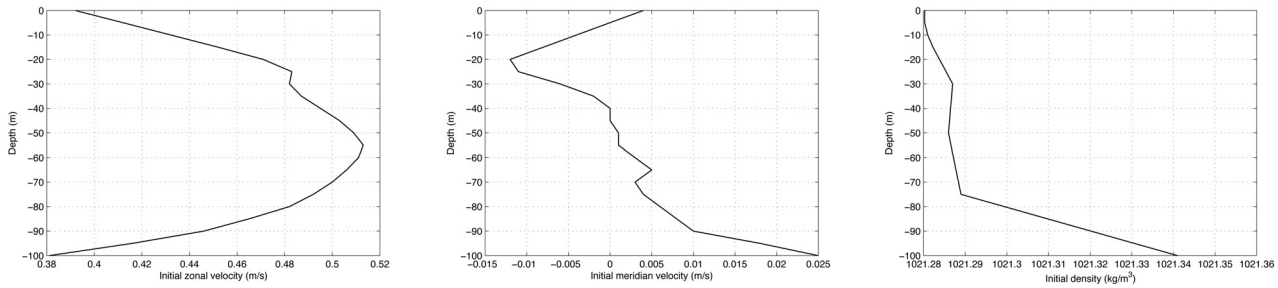

FIGURE 9. The initial profiles for zonal velocity, meridian velocity and density (from left to right).

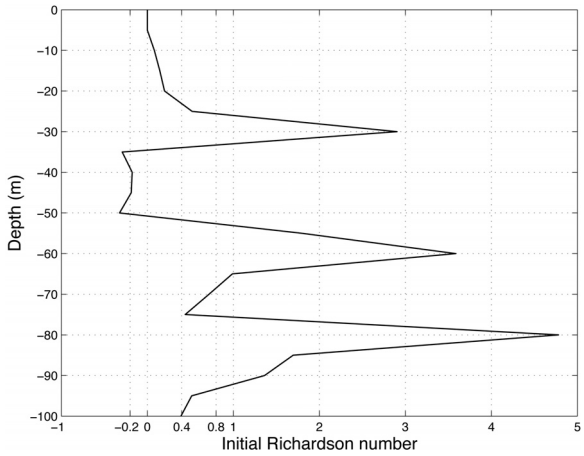

FIGURE 10. Initial Richardson numbers, corresponding to the initial profiles of Figure 9.

This is not an isolated situation, as the TAO data show similar instability zones for several days between the 16th and the 22th November 1991.

As we may observe in Figure 10, the initial Richardson number R^0 is negative in the depth range $[-50\text{ m}, -30\text{ m}]$, taking values smaller than $R^0 = -0.2$ at $z = -45$ m. The PP and Gent models yield negative turbulent diffusions for these data, and can not be run. In its turn, our new model has positive diffusivity for all values of the Richardson number.

The new model is integrated for 48 h. We present the results corresponding to $\Delta z = 5$ m, and $\Delta t = 60$ s, with boundary conditions $u_1 = 11.7\ \text{m}\cdot\text{s}^{-1}$ (eastward wind), $u_2 = 0.4\ \text{m}\cdot\text{s}^{-1}$ (northward wind) and buoyancy flux $Q = -1 \times 10^{-6}\ \text{kg}\cdot\text{m}^{-2}\cdot\text{s}^{-1}$ ($\simeq -11\ \text{W}\cdot\text{m}^{-2}$).

The results are displayed in Figure 11. Our model produces a homogeneous seventy meters deep mixed layer, with a structure quite similar to test Case 1, where the initial density presented a stable configuration. The density remains almost constant down to $z \simeq -70$ m, and presents a pycnocline immediately below. The profiles for velocities are quite smooth, as correspond to a well-mixed layer.

7. Analysis of a simplified model

To illustrate the ability of Potier-Ferry's theory to analyze our model equations (2.2) in the neighborhood of equilibrium solutions, we present the analysis of a simplified model for one single unknown. This unknown may be viewed as the equation satisfied by the unknown ρ in system (2.2) once the velocity field is known.

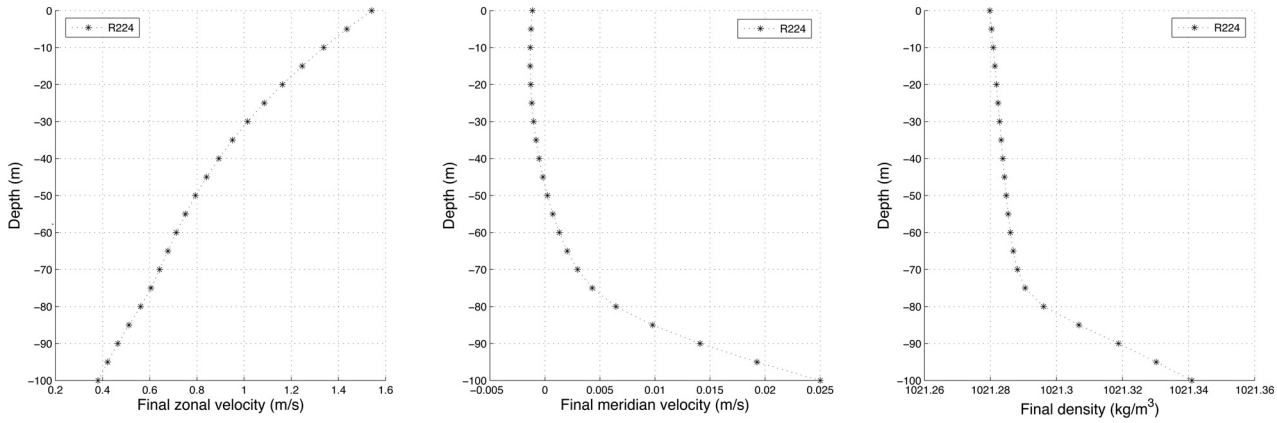

FIGURE 11. Profiles for zonal velocity, meridian velocity and density (from left to right) computed with the new model.

This model reads

$$\partial_t \rho - \partial_z (f(\partial_z \rho)\partial_z \rho) = 0, \tag{7.1}$$

$$f(\partial_z \rho)\partial_z \rho|_{z=0} = Q_s,\ f(\partial_z \rho)\partial_z \rho|_{z=-h} = Q_b, \tag{7.2}$$

$$\rho(0) = \rho_0. \tag{7.3}$$

Here, $f(\theta)$ stands for the turbulent diffusion. We assume that this is a real function given by

$$f(\theta) = \alpha + \frac{\beta}{(1-\gamma\,\theta)^m}, \quad \text{for some } \alpha > 0,\ \beta > 0,\ \gamma > 0,\ m > 0, \quad \text{for } \theta < 0. \tag{7.4}$$

This is a function with the same structure of the turbulent diffusions appearing in PP and Gent models, if we replace the Richardson number R by $\theta = \partial_z \rho$. Negative values of θ correspond to stable vertical configurations. For positive θ, that correspond to unstable configurations, we may assume that f is increasing: for larger θ the water column is more unstable, and then the turbulent diffusion also must be larger.

We are interested in finding an equation for $\theta = \partial_z \rho$. This equation is formally obtained by deriving (7.1) with respect to z:

$$\partial_t \theta - \partial_z \left[(f(\theta) + f'(\theta)\,\theta)\,\partial_z \theta \right] = 0. \tag{7.5}$$

This appears as a non-linear parabolic equation with diffusion

$$g(\theta) = f(\theta) + f'(\theta)\,\theta.$$

So we consider the problem

$$\partial_t \theta - \partial_z \left[g(\theta)\,\partial_z \theta \right] = 0 \quad \text{in } (-h, 0) \times (0, +\infty), \tag{7.6}$$

$$\theta|_{z=0} = \theta_s,\ \theta|_{z=-h} = \theta_b \quad \text{in } (0, +\infty), \tag{7.7}$$

$$\theta(0) = \theta_0 = \partial_z \rho_0 \quad \text{in } (-h, 0). \tag{7.8}$$

Here we set Dirichlet boundary conditions for θ deduced from the Neumann boundary conditions (7.2). We assume that the equation $f(\theta)\,\theta = Q_s$ admits a unique solution $\theta = \theta_s$, that we set as Dirichlet boundary

condition at $z = 0$. Notice that, by the Implicit Function Theorem, this will hold in the set of θ for which $g(\theta) = f(\theta) + f'(\theta)\,\theta \neq 0$. And similarly at $z = -h$.

We are interested in analyzing whether problem (7.6)–(7.8) is well posed, at least for initial and boundary data in a neighborhood of equilibria states, and whether these equilibria states are stable.

Notice that the equilibria states of equation (7.6) that we are interested in are those associated to equation (7.1). By (3.5), these equilibria are given by,

$$\rho^e(z) = \rho_b + \frac{Q}{f\,(R^e)}\;(z+h)\,;$$

where the equilibrium Richardson number R^e is given. So we shall be interested in equilibria of equation (7.6) given by

$$\theta^e(z) = \frac{Q}{f\,(R^e)}. \tag{7.9}$$

It is obvious that such a constant function is an equilibrium of equation (7.6). However, we write it in this way to make apparent its relationship with the heat flux Q. Indeed, we next prove that a wide range of *negative* equilibria are stable. This corresponds to negative heat flux Q, and then to physically stable configurations of the oceanic boundary layer. So we recover a meaningful consistence between physical and mathematical stability of this layer for the simplified model considered.

Our analysis is specifically based upon Theorem 3 of in Potier-Ferry's work [15]. Although this theorem applies to more general systems of equations, to avoid unnecessary complexities we state it for non-linear parabolic equations of the form

$$\partial_t u = a(u, \partial_z u)\,\partial_{zz} u + b(u, \partial_z u) \quad \text{in } \Omega \times [0,T], \tag{7.10}$$

$$u(x,t) = 0 \quad \text{on } \partial\Omega \times [0,T], \tag{7.11}$$

$$u(x,0) = u_0(x) \quad \text{on } \Omega; \tag{7.12}$$

where Ω is a bounded open subset of $\mathbb{R}$. Theorem 3 of [15] for system (7.10)–(7.12) reads as follows:

Theorem 7.1. *Let the functions $(u,G) \mapsto a(u,G)$, $b(u,G)$ be defined for (u,G) in a neighborhood of 0 in $\mathbb{R}\times\mathbb{R}$. Let $\eta > 0$ be a number such that the function $(u,G) \mapsto a(u,G)$ is in $C^{1,\eta}$ and assume that the function $(u,G) \mapsto b(u,G)$ is in C^2. Assume that $a(0,0)$ is positive.*

If $p > 1$, if the initial data are sufficiently small in $W^{2,p}(\Omega)$, and if the initial data vanish on $\partial\Omega$, then system (7.10)–(7.12) has a unique solution in the class

$$C([0,t_0], W^{2,p}(\Omega)) \cap C^1([0,t_0], L^p(\Omega))$$

for some $t_0 > 0$.

Furthermore, if $u = 0$ satisfies (7.10) and if all the solutions of the linearized equation decay exponentially, then the solution of (7.10)–(7.12) exists for all positive times t and the equilibrium state $u = 0$ is exponentially stable with respect to the $W^{2,p}$ norm.

From this result we deduce:

Theorem 7.2. *Assume that function f is of class C^3 in a neighborhood of an equilibrium solution $\theta \equiv \theta^e$. Assume $g(\theta^e) > 0$. Assume finally that the Dirichlet boundary conditions in problem (7.6)–(7.8) are*

$$\theta_s = \theta^e,\ \theta_b = \theta^e.$$

Then, if the datum θ_0 is close enough in $W^{2,p}([-h,0])$ to θ^e for some $p > 1$, problem (7.6)–(7.8) admits a unique solution in

$$C([0,+\infty), W^{2,p}(-h,0)) \cap C^1([0,+\infty), L^p(-h,0)).$$

Furthermore, the equilibrium θ^e is exponentially stable with respect to the $W^{2,p}$ norm.

Proof. We at first re-write problem (7.6)–(7.8) in terms of the variable $u = \theta - \theta^e$ that satisfies homogeneous Dirichlet boundary conditions. Equation (7.6) reduces to equation (7.10) with

$$a(u, G) = g(u + \theta^e),$$

$$b(u, G) = \partial_z g(u + \theta^e)(G + \partial_z \theta^e) + g(u + \theta^e)\, \partial_{zz}\theta^e - \partial_z \left(g(\theta^e)\, \partial_z \theta^e\right)) = \partial_z g(u + \theta^e)\, G.$$

As f is of class C^3 in a neighborhood of θ^e, then a and b are of class C^2 in the same neighborhood.

As $g(\theta^e) > 0$, by Theorem 7.1, if $\theta_0 - \theta^e$ is small enough in $W^{2,p}([-h, 0])$, there exists a unique solution of (7.6)–(7.8) in $C([0, t_0], W^{2,p}([-h, 0])) \cap C^1([0, t_0], L^p([-h, 0]))$, for some $t_0 > 0$.

Also, the linearized equation(7.6) at $\theta = \theta^e$ is

$$\partial_z \theta' - g(\theta^e)\, \partial_{zz}\theta' = 0,$$

where θ' is a perturbation of θ^e. As $g(\theta^e) > 0$, the solutions of this equation decay exponentially as $t \to +\infty$. Then, by Theorem 7.1, the above solution θ exists in $(0, +\infty)$ and decays exponentially to the equilibrium solution θ^e as $t \to +\infty$. □

Consequently, the global existence and stability of solutions of problem (7.6)–(7.8) is restricted to the only condition $g(\theta^e) > 0$. Notice that for $0 < m \leq 1$, g is an increasing function, and $g(\theta) \geq \alpha$, $\forall \theta \leq 0$. However, for $m > 1$, g is negative in a range of negative θ. Indeed, g attains its minimum at $\theta_m = -\dfrac{2}{(m-1)\,\gamma}$ with value

$$g(\theta_m) = \alpha - \beta \left(\frac{m-1}{m+1}\right)^{m+1}.$$

For the physical values of α and β appearing in PP and Gent models, this value is negative. Thus, in general we may ensure that the equilibrium solution θ^e is stable only if θ^e lays in the range of negative θ for which $g(\theta) > 0$. As $\lim_{t \to -\infty} g(\theta) = +\infty$ and $g(0) > 0$, we conclude that all negative equilibria but those laying in a compact set are stable.

Notice that the theory of Potier-Ferry [15] only applies to homogeneous Dirichlet boundary conditions. This is the reason why we have changed the problem (7.1)–(7.3) for ρ, that contains non-linear Neumann boundary conditions, into problem (7.6)–(7.8) for the variable $\theta = \partial_z \rho$, that contains Dirichlet boundary conditions. However, we cannot consider the actual analysis as totally satisfactory for the simplified problem (7.1)–(7.3), as there is a range of negative equilibrium states θ^e, which corresponds to physically stable configurations, whose mathematical stability we are not able to prove. This could be intrinsic, or due to the re-formulation of problem (7.1)–(7.3) into problem (7.6)–(7.8). A (quite technical) adaptation of this theory would be needed to deal with the full problem (2.2), including non-linear Neumann boundary conditions for velocity and density.

We think that the preceding analysis of the simplified model (7.6)–(7.8) gives a taste of what can be done if Potier-Ferry's theory is correctly extended to problem (2.2). Notice that $f(\theta^e) > 0$ for all negative equilibria θ^e. This gives some hope that all negative equilibria are mathematically stable. Even there is hope that the equilibria of the full problem (2.2) are stable, as it is linearly stable as we have proved.

8. Conclusions

In this paper we have analyzed from the mathematical point of view several relevant questions related to algebraic turbulence models for oceanic turbulent mixing layers.

We have proved that the equilibria of these models are linear profiles for velocity and density, and that these are linearly stable. We have performed some numerical tests that show that these profiles are indeed asymptotically reached by the usual numerical methods that solve the continuous models. These tests also have shown that the mixing-layer configurations are transient states of the flow, that asymptotically converge to equilibria.

We also have proved a stability result on a finite-difference numerical method usually employed to solve algebraic mixing-layer models. The numerical tests show the ability of this numerical method to reproduce mixing-layers and theoretical equilibria.

We also have justified and interpreted these results in the framework of Potier-Ferry's theory on the application of the linearization principle to non-linear parabolic equations. The interest of studying the equilibria states is justified as exponential linear stability implies non-linear stability. Also, mixing-layer configurations appear as states that belong to the domain of attraction of equilibria. Further, we have analyzed a simplified model for which Potier-Ferry's theory yields the asymptotic stability of a large range of physically stable equilibria. This justifies the use of this theory as guideline to develop this study.

A further analysis would require the extension of Potier-Ferry theory to non-linear Neumann boundary conditions. This seems technically reachable, by fixed-point linearisation techniques. This would prove the non-linear exponential stability of the equilibria introduced in the present paper.

Another relevant question still open is the analysis of convergence of finite-difference numerical solvers. This requires the obtention of estimates in $W^{2,p}$ of the approximated solutions. It could also be proved by a suitable extension of semigroup theory, that would prove the convergence to continuous solutions close enough to some equilibrium.

A further step would be the analysis of existence of solutions for stable configurations: $\partial_z \rho \leq 0$, not necessarily close to an equilibrium solution. In the opinion of the authors, this would need the development of a new theory.

Acknowledgements. Research of T. Chacón Rebollo and M. Gómez Mármal partially funded by Spanish DIG grants MTM2006-01275 and MTM2009-07719. R. Lewandowski warmly thanks the Departamento de Ecuaciones Diferenciales y Análsis Numérico of the University of Sevilla for frequent hospitality. Research of R. Lewandowski partially supported by ANR contract 08FA300-01.

References

[1] B. Blanke and P. Delecluse, Variability of the tropical atlantic ocean simulated by a general circulation model with two different mixed-layer physics. *J. Phys. Oceanogr.* **23** (1993) 1363–1388.
[2] J.H. Bramble, J.E. Pasciak and O. Steinbach, On the stability of the l^2 projection in h^1. *Math. Comp.* **7** (2001) 147–156.
[3] H. Burchard, *Applied turbulence modelling in marine water*. Ph.D. Thesis, University of Hambourg, Germany (2004).
[4] P. Gaspar, Y. Gregoris and J.-M. Lefevre, A simple eddy kinetic energy model for simulations of the oceanic vertical mixing: test at Station Papa and long-term upper ocean study site. *J. Geophys. Res.* **16** (1990) 179–193.
[5] P.R. Gent, The heat budget of the toga-coare domain in an ocean model. *J. Geophys. Res.* **96** (1991) 3323–3330.
[6] H. Goosse, E. Deleersnijder, T. Fichefet and M.H. England, Sensitivity of a global coupled ocean-sea ice model to the parametrization of vertical mixing. *J. Geophys. Res.* **104** (1999) 13681–13695.
[7] J.H. Jones, Vertical mixing in the equatorial undercurrent. *J. Phys. Oceanogr.* **3** (1973) 286–296.
[8] Z. Kowalik and T.S. Murty, *Numerical modeling of ocean dynamics*. World Scientific (1993).
[9] W.G. Large, C. McWilliams and S.C. Doney, Oceanic vertical mixing: a review and a model with a nonlocal boundary layer parametrization. *Rev. Geophys.* **32** (1994) 363–403.
[10] G. Madec, P. Delecluse, M. Imbard and C. Levy, *OPA version 8.0, Ocean General Circulation Model Reference Manual*. LODYC, Int. Rep. 97/04 (1997).
[11] M. McPhaden, The tropical atmosphere ocean (tao) array is completed. *Bull. Am. Meteorol. Soc.* **76** (1995) 739–741.
[12] G. Mellor and T. Yamada, Development of a turbulence closure model for geophysical fluid problems. *Rev. Geophys. Space Phys.* **20** (1982) 851–875.
[13] R.C. Pacanowski and S.G.H. Philander, Parametrization of vertical mixing in numericals models of the tropical oceans. *J. Phys. Oceanogr.* **11** (1981) 1443–1451.
[14] J. Pedloski, *Geophysical fluid dynamics*. Springer (1987).
[15] M. Potier-Ferry, The linearization principle for the stability of solutions of quasilinear parabolic equations. *Arch. Ration. Mech. Anal.* **77** (1981) 301–320.
[16] A.R. Robinson, An investigation into the wind as the cause of the equatiorial undercurrent. *J. Mar. Res.* **24** (1966) 179–204.